

Biophysics / Biophysique

In situ measurements of viral particles diffusion inside mucoid biofilms

Pascaline Lacroix-Gueu^a, Romain Briandet^b, Sandrine Lévêque-Fort^a,
Marie-Noëlle Bellon-Fontaine^b, Marie-Pierre Fontaine-Aupart^{a,*}

^a Laboratoire de photophysique moléculaire, UPR 3361, fédération LUMAT, université Paris-Sud, 91405 Orsay, France

^b Unité de recherche en bioadhésion et hygiène des matériaux, INRA UBHM, av. de la République, 91300 Massy, France

Received 28 September 2005; accepted 30 September 2005

Available online 2 November 2005

Presented in the framework of the European Workshop on Fluorescence Correlation – Spectroscopy Techniques Applications in Biology, Medicine and Pharmacology, Faculty of Medicine of Paris-Sud, Le Kremlin-Bicêtre, France, 24 & 25 March 2005

Presented by Jean Rosa

Abstract

Fluorescence correlation spectroscopy (FCS) under two-photon excitation was used successfully to characterize the diffusion properties of model virus particles (bacteriophages) in bacterial biofilm of *Stenotrophonas maltophilia*. The results are compared to those obtained with fluorescent latex beads used as a reference. The FCS data clearly demonstrated the possibility for viral particles to penetrate inside the exopolymeric matrix of mucoid biofilms, and hence to benefit from its protective effect toward antimicrobials (antibiotics and biocides). Microbial biofilms should hence be considered as potential reservoirs of pathogenic viruses, and are probably responsible for numerous persistent viral infections. **To cite this article:** P. Lacroix-Gueu et al., C. R. Biologies 328 (2005).

© 2005 Académie des sciences. Published by Elsevier SAS. All rights reserved.

Résumé

Mesure in situ de la diffusion de particules virales à l'intérieur de biofilms mucoïdes. La spectroscopie de corrélation de fluorescence (FCS) sous excitation à deux photons a été utilisée avec succès pour caractériser les propriétés de diffusion de particules virales modèles (bacteriophages) dans un biofilm bactérien de *Stenotrophonas maltophilia*. Les résultats ont été comparés avec ceux obtenus pour des billes de latex fluorescentes utilisées comme référence. Les données obtenues en FCS démontrent la possibilité pour une particule virale de pénétrer dans la matrice exopolymérique de biofilms mucoïdes, et de bénéficier ainsi d'un environnement protecteur vis-à-vis d'agressions extérieures telles que l'action d'agents antimicrobiens (antibiotiques ou désinfectant). Les biofilms peuvent ainsi être considérés comme des réservoirs potentiels de virus pathogènes, et sont probablement impliqués dans de nombreuses infections virales persistantes. **Pour citer cet article :** P. Lacroix-Gueu et al., C. R. Biologies 328 (2005).

© 2005 Académie des sciences. Published by Elsevier SAS. All rights reserved.

Keywords: FCS; Fluorescence; Bacterial biofilms; Phages; Viruses

Mots-clés: FCS; Fluorescence; Biofilms bactériens; Phages; Virus

* Corresponding author.

E-mail address: marie-pierre.fontaine-aupart@ppm.u-psud.fr (M.-P. Fontaine-Aupart).

1. Introduction

Surfaces exposed to non-sterile and wet environments can be colonized by adherent microorganisms that engage themselves in hydrated exopolymeric substances (EPS) containing mainly polysaccharides, proteins and nucleic acids, forming a slimy layer known as a biofilm [1]. In medical medium, bacterial biofilms are able to colonize various surfaces (walls, floors, surgical tables, etc.) or implanted medical devices (catheters, endoscopes, pacemakers...), and are responsible for about 65% of nosocomial infections by direct infection or transmission [2,3].

Biofilms are characterized by a high level of structuration, most likely correlated to their specific function and their stability. Indeed, bacteria embedded in biofilms present specific physiological and genetic features that differentiate them from their planktonic counterparts [4]. Furthermore, biofilms are highly heterogeneous, with structures such as streamers and water channels, depending on the prevailing conditions, environmental stresses and EPS nature, which create a vascularization system similar to animal tissue. The biofilm depth can vary from a few micrometres up to centimetres depending on the strain and the environment.

The physicochemical and structural natures of EPS influence the bacterial physiology [5], but also may act to various degrees as a protection against environmental changes, such as desiccation or action of antimicrobials (antibiotics and biocides). Moreover, these exopolymers have been frequently invoked to account for the development of anaerobic micro-zones and structural heterogeneity in biofilms and thus may also act as a reservoir for pathogenic viral particles [6], leading to persistent viral infection.

Thus measuring the diffusive capabilities of various chemical species within the biofilm matrix is of importance to understand the dynamics of these microbial communities and to identify the role and function of EPS. Such studies have been first approached by means of scanning confocal laser microscopy (SCLM) combined with fluorescence recovery after photobleaching measurements (FRAP) [5]. However, FRAP does not allow a direct visualization of the fluorophore diffusion inside the excited volume and requires high fluorophore concentrations that can lead to inaccuracy in the diffusion coefficient determination [7]. More recently, we have demonstrated for the first time that fluorescence correlation spectroscopy (FCS) under two-photon excitation (TPE) can be successfully applied to characterize the penetration and diffusion capabilities of fluorescent tracer particles in monomicrobial biofilms [8].

FCS, based on the analysis of fluctuation intensities in the fluorescence signals emitted by a small number of molecules in a microvolume, is ideally suited for non-invasive in vivo measurements [9]. By comparison with conventional one-photon FCS, TPE minimizes photobleaching in spatially restricted volumes (~1 femtolitre), thereby preventing long-term signal acquisition and measurement with single molecule sensitivity. Furthermore, the use of infrared wavelengths ensures deeper penetration than SCLM.

In this work we analyse the role of the *Stenotrophonas maltophilia* biofilm structure and specially the influence of EPS towards the diffusion and reactivity of bacteriophages. These viral particles also named phages are considered as favoured model for human enteric virus due to their similarity of structure, size, composition and morphology as well as behaviour toward conventional water treatment processes. The model viral particle used in this study was a C2 bacteriophage known to recognize specific surface sites of *Lactococcus lactis* subsp. *lactis* bacteria lacking on *Stenotrophonas maltophilia* cells. *Stenotrophonas maltophilia* is an aerobic bacillus of growing clinical importance [10] because it is the third bacteria involved in nosocomial infections after *Pseudomonas aeruginosa* and *Staphylococcus aureus*. This microorganism, when grown as a biofilm, contains mucoid mushroom-like structure typical of many gram negative bacteria [11], and is known to be particularly resistant to antimicrobials.

2. Materials and methods

2.1. Bacterial biofilms in continuous flow cells

This study was carried out with the bacterial strain *Stenotrophonas maltophilia* 114N-Sm provided by UNIR association (<http://www.unir.org>). The strain was stored at -20°C , transferred twice in TSB (Tryp-case Soy Broth, BioMérieux) before being cultivated overnight in 100 ml of TSB in continuous flow slide culture at 30°C under oxygenated conditions.

Bacterial cells in stationary phase were washed by a succession of three centrifugations (7000 g, 4°C , 10 min) and resuspensions in 150 ml NaCl. Bacterial concentration was adjusted to 10^9 CFU/ml by measurements of the absorbance ($A_{400\text{ nm}} = 0.8$). Two millilitres of the suspension were poured into a flow cell (BST FC81, Biosurface Technology, Bozeman, USA) with a sterile syringe. In this experimental setup, the biofilms grow up on the glass cover slit of the flow cell ($0.17 \times 24 \times 60$ mm). After 3 h of static adhe-

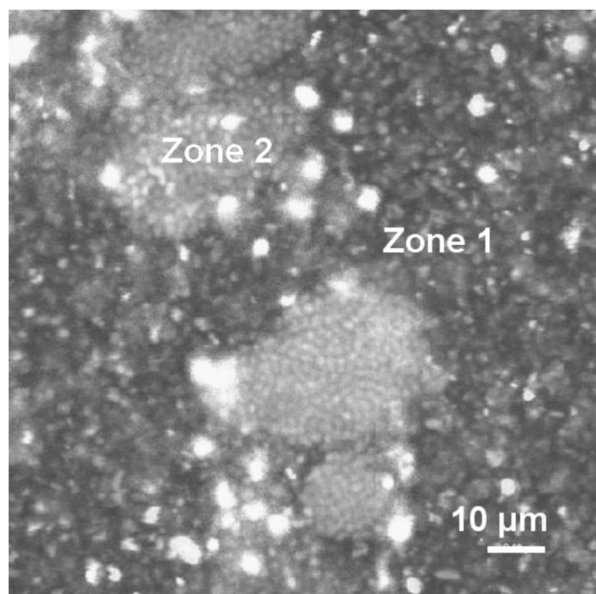


Fig. 1. Confocal imaging of *Stenotrophonas maltophilia* biofilm showing (zone 1) unstructured and (zone 2) mushroom-like structure.

sion in NaCl 150 mM, a bulk laminar flow rate of 0.5 ml min^{-1} of growth medium (TSB 1:10) crosses the flow cell in order to eliminate planktonic cells, to allow adherent bacteria to multiply and to form a biofilm (flow obtained from a Watson and Marlow 205S peristaltic pump). The biofilm development period in dynamic conditions prior to FCS experiments was always 24 h at 20°C in order to minimize bacterial physiological variations in the biofilm structure and thus artefacts in the FCS measurements. *Stenotrophonas maltophilia* biofilms (Fig. 1) have been extensively studied and represent well-defined systems with mushroom-like structure (zone 2) of $\sim 30\text{-}\mu\text{m}$ thickness separated by homogeneous layers of bacteria (zone 1) of less than $10 \mu\text{m}$. Biofilm depth was determined manually using the computer-controlled focusmeter of a SCLM system (TCS SP2, Leica Microsystems, France) and defined with respect to the cover slit surface (i.e. at the attachment of the biofilm); the top layer of the biofilm ($\sim 30 \mu\text{m}$ from the glass cover slit) corresponds to the interface with the flowing growth medium.

2.2. Prolate bacteriophages

The model viral of particle used in this study was a C2 bacteriophage infecting *Lactococcus lactis subsp. lactis*. The 22163-bp genome of this lactococcal phage was fully sequenced [12]. The C2 phage exhibits a prolate structure with a 100-nm head and a 200-nm non-contractile tail. *Lactococcus lactis* was cultivated when

necessary in M17 growth medium (Oxoid, France) supplemented with 0.5% of glucose and incubated at 30°C overnight. Phage C2 and the C2-sensitive strain *Lactococcus lactis*, subsp. *lactis* were provided by S. Kulakauskas (INRA URLGA, Jouy-en Josas).

Phage titration was performed using the serial dilution technique and the formation of lytic plaques on a layer of the sensitive bacteria on a Petri dish, as described previously [13]. Experimentally, 0.1 ml of the phage suspension was added to 0.2 ml of a mid-log-phase bacterial culture of the C2-sensitive bacteria *L. lactis*. $30 \mu\text{l}$ of CaCl_2 1 M were added to favour phage infection, and the mixture was incubated 10 min at 30°C . Each mixture was added to 3 ml of soft agar (M17 Oxoid supplemented with 8 g l^{-1} of agar and 0.5% of glucose) in order to create a soft double layer on agar plates (M17 Oxoid supplemented with 15 g l^{-1} of agar and 0.5% of glucose). Petri dishes were incubated overnight at 30°C in order to enumerate the visible lytic plaques.

For phage amplification, 10^8 PFU (Plaque Forming Units) of phage C2 were added to 400 ml of a *L. lactis* culture ($\text{DO}_{600 \text{ nm}} = 0.1$). Infected bacterial cells were incubated at 30°C until clearance of the suspension. The mixture was then centrifuged to eliminate bacterial debris for 10 min at $7000 g$ and 4°C . Phage particles were then washed in NaCl 150 mM by a centrifugation at $18000 g$ for 6 h. The pellet was resuspended in 10 ml of 150 mM NaCl and sterilized by filtration ($0.22 \mu\text{m}$, Steriflip, Millipore). The final phage suspension titrated 10^{10} PFU/ml was stored at 4°C .

2.3. Fluorescent probes

The anionic carboxylate-modified fluorescent latex beads of 110-nm diameter (range size of bacteriophage head), obtained from Molecular Probes were used as reference. The beads were used in suspension in deionised water (Purit, France). The solutions were filtered and sonicated before each experiment in order to eliminate most of the aggregates and to obtain a final concentration from 1 nM (in solution) to 10 nM (in biofilms). The latex beads could be considered to have a globular structure, enabling an estimation of their diffusion coefficient using the Stokes equation.

The selection criteria for bacteriophage fluorescent labelling were imposed by the experimental conditions required for FCS under TPE: (i) the fluorophore must be excited by two photons in the wavelength range 700–900 nm; (ii) detection of the fluorescence signal emitted during the counting interval needed to be significant despite the low excitation energy and the low fluorophore

concentration used, which required to use a fluorophore with a significant fluorescence quantum yield; (iii) the fluorophore must be able to label the bacteriophage and not the living cells inside the biofilms. Because of these constraints, the fluorescent probe used to label the C2 bacteriophage was Sytox green (Molecular probes). The maximal concentration of labelled bacteriophages was obtained by adding 30 μl of Sytox green (5 mM solution) to 5 ml of C2 bacteriophage suspension titrated at 10^{10} PFU ml^{-1} . The excess of free Sytox green was removed by careful rinsing. The labelled bacteriophage solution was used as it was for FCS measurements in biofilms and diluted by a factor 10 for experiments in solution. Before the FCS measurements inside biofilms, the growth medium flow was stopped and 2 ml of fluorophores were injected aseptically through the flow cell.

2.4. FCS set-up

The TPE experimental system used in this study has been described in detail elsewhere [14]. Briefly, the fluorescence excitation source was a femtosecond Ti:Sapphire laser (MIRA 900, Coherent Inc., Santa Clara, CA) pumped in the green by a continuous-wave diode-pumped solid-state laser (VERDI, Coherent Inc.) generating 100-fs pulses at a 76-MHz repetition rate with about 700-mW average power output. An excitation wavelength of 890 nm was fixed for all of the TPE experiments described here. The laser beam is expanded 3 times at the entrance of the microscope in order to reach a diameter of approximately 5 mm in diameter to fill the back aperture of the objective. After the beam expander, parallel laser light epi-illuminates a Zeiss 63×1.4 numerical aperture, oil immersion objective. Fluorescence emission was collected through the same objective, separated from the excitation radiation by a dichroic mirror. It was then filtered through short-pass filters to absorb any possible diffused infrared excitation light and focused on the surface of a photomultiplier tube (R7205-01, Hamamatsu, Massy, France). This device was connected to a discriminator (TC 454, Oxford Instruments Inc., Oxford, UK), and the output signal was transmitted to a digital autocorrelator module (Flex2kx2-12, correlator) that computes on-line the correlation function of the fluorescence fluctuations. To measure translational diffusion time with 10 to 20% (see below) accuracy, data recording times are 60–100 s for solution acquisitions and 100–300 s in the biofilms and corresponds to 10–20 iterations, respectively. The data are stored in the computer and analysed by a home-written routine that allows to: (i) select and average cho-

sen successive acquisitions, (ii) make anomalous diffusion fit if necessary (see below), (iii) calculate the associated standard deviations.

A general concern in fluorescence microscopy measurements and especially for applications with slow moving particles through biofilm depth is the risk of photobleaching the fluorophores at high laser power values. For this reason, we always used less than 1 mW at the sample and thus no cellular degradation was observed during the time of experiments as verified by confocal microscopy with the live/dead bacterial viability kit (Molecular probes). Furthermore, while IR excitation wavelength was used (890 nm), no significant temperature increase due to water absorption was observed.

2.5. FCS diffusion analysis

The conceptual and theoretical basis of FCS has been well established [7,9,15,16]. Assuming that the excitation intensity profile could be approximated using a three-dimensional Gaussian distribution, the fluorescence correlation curves in the case of free Brownian motion of molecules can be fitted using the following normalized autocorrelation function:

$$g(\tau) = 1 + \left(\frac{1}{\sqrt{8N}} \right) \left(\frac{1}{1 + (\tau/\tau_D)} \right) \times \left(\frac{1}{1 + (\omega_0/z_0)^2(\tau/\tau_D)} \right)^{1/2} \quad (1)$$

N denotes the mean number of fluorescent molecules in the excitation volume (it must be noted that fluorescence correlation measurements required low N values to allow detection); ω_0 is the beam-waist at the focal point and z_0 the focal depth. Previous calibration experiments, using 50 nm radius spheres ($D = 4 \mu\text{m}^2 \text{s}^{-1}$) diffusing in water enabled us to determine a ω_0 value of $0.52 \pm 0.02 \mu\text{m}$ and $\omega_0/z_0 = 0.3 \pm 0.01$ [14].

Under biphotonic excitation, the translational diffusion time can be related to the beam waist ω_0 and the diffusion coefficient D_t of the fluorophore by the relation:

$$\tau_D = \omega_0^2/8D_t \quad (2)$$

For approximately spherical particles (such as latex beads) of hydrodynamic radius (R), the local viscosity η of the medium can be obtained via the Stokes–Einstein equation:

$$\eta = \frac{4kT\tau_D}{3\pi R\omega_0^2} \quad (3)$$

In the presence of obstacles that lead to deviation of the molecules from Brownian motion (called anomalous diffusion) [7], the normalized autocorrelation function is transformed into:

$$g(\tau) = 1 + \left(\frac{1}{\sqrt{8N}} \right) \left(\frac{1}{1 + (\tau/\tau_D)^{2/d_w}} \right) \times \left(\frac{1}{1 + (\omega_0/z_0)^2 (\tau/\tau_D)^{2/d_w}} \right)^{1/2} \quad (4)$$

The parameter d_w is equal to 2 for free diffusion and increases with increasing obstacle concentration. This results in an increase of the translational diffusion time, τ_D , and to a decrease of the apparent diffusion coefficient, D_t .

3. Results and discussion

The main goal of this work was to demonstrate the possibility of investigating the influence of biofilm structure on viral particle diffusion using FCS under TPE.

The diffusion processes were characterized by comparing the fluorescence correlation curves measured for C2 bacteriophages in solution and integrated into the *Stenotrophonas maltophilia* biofilm. As a reference, FCS measurements were also performed using reference anionic latex beads.

3.1. Solution measurements

Typical experimental fluorescence correlation curves obtained in aqueous solutions at room temperature (water viscosity $\eta_w = 0.96$ cP at 295 K) for latex beads and free fluorescent labelled bacteriophages are shown in Fig. 2. The τ_D and N values are obtained by fitting the experimental curves considering Brownian motion diffusion (Eq. (1)). The corresponding diffusion coefficients (D) calculated using Eq. (2) were $3.1 \mu\text{m}^2 \text{s}^{-1}$ and $1.2 \mu\text{m}^2 \text{s}^{-1}$ for the carboxylate beads and the viral particles, respectively. It can be observed that this D value is ~ 2.6 time lower for the bacteriophage compared to fluorescent beads revealing that the exocellular tail of the viral particle significantly reduces its mobility.

Moreover, the experimental diffusion coefficient measured for the fluorescent microspheres is in good agreement with the theoretical value (D_0) expected from the Stokes–Einstein equation ($D_0 = 4.0 \mu\text{m}^2 \text{s}^{-1}$), a result that demonstrates the accuracy of our FCS technique.

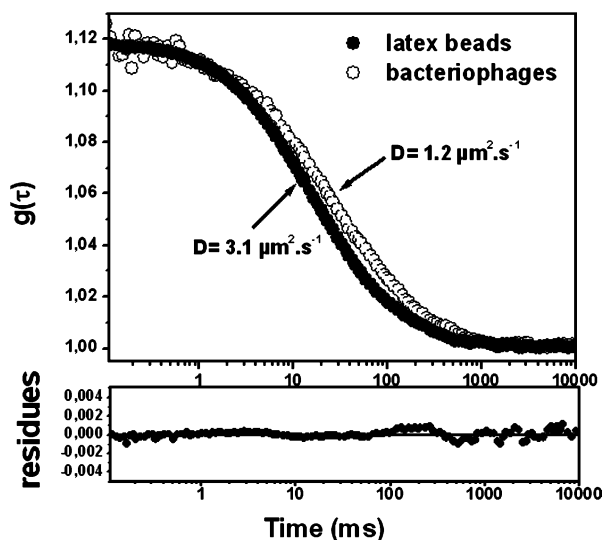


Fig. 2. Experimental fluorescence correlation curves $g(\tau)$ corresponding to (●) anionic latex beads of 55-nm radius and (○) fluorescent labelled C2 bacteriophages in water. Continuous lines correspond to the fitting of the curves using Eq. (1). Parameters obtained from fit are: $N = 1.5$, $\tau_d = 11.2$ ms for the latex beads and $N = 5.8$, $\tau_d = 28.6$ ms for the phages. Standard deviation was 5% of the values.

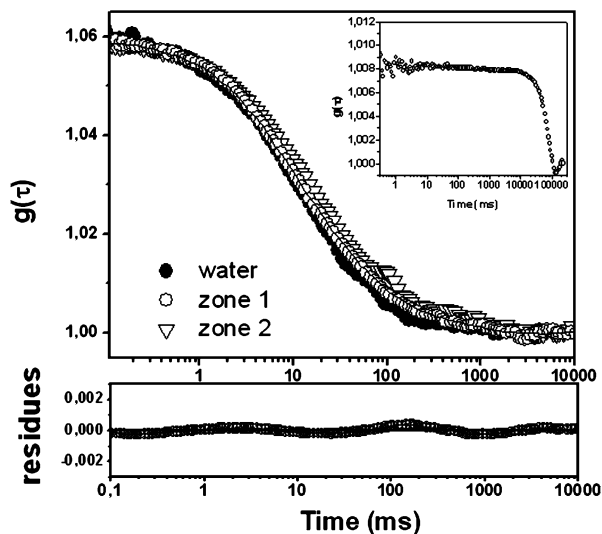


Fig. 3. Fluorescence correlation curves for the anionic latex beads obtained in water and in the two distinct structural zones of *Stenotrophonas maltophilia* biofilm. The fitting of the curves was obtained using Eq. (1) in water (●) and zone 1 (○) and with Eq. (4) for the more distorted curve in zone 2 (▽).

3.2. Application of FCS to microbial biofilms

We have observed that, in our experimental conditions, the bacterial autofluorescence as well as the overall biofilm movement were able to create a correlation signal (Fig. 3, inset). However, the translational diffu-

sion coefficient associated to this background movement ($\tau_D > 50$ s) was out of range compared to the τ_D values obtained for the fluorescent probes ($\tau_D < 150$ ms) and thus did not interfere with the fluorophore diffusion.

3.2.1. Latex beads

The differences of mobility of the anionic latex beads at different horizontal positions within the *S. maltophilia* biofilm are apparent in Fig. 3: the FCS measured in zone 1 (more homogenous structure) can be fitted using Eq. (1), while the FCS recorded in zone 2 (mushroom-like structure) requires an anomalous diffusion model (Eq. (4)) for interpretation.

In zone 1, we found a mean τ_D value of 13 ms corresponding to a diffusion coefficient of $2.6 \mu\text{m}^2 \text{s}^{-1}$ and to a local viscosity of the medium of $\eta = 0.81$ cP (Eq. (3)). This value is in the same order as in water, revealing that the local viscosity through the homogenous structure of the biofilm is not very different from that of water. This result is in agreement with previous observations that describe biofilms as open architectures in which the biomass is interspersed with channels of lower density, such as water channels [17].

Because of the complex nature of biofilms, it is necessary to rule out any artefacts before the diffusion can be termed truly anomalous. In particular, the diffusion rates can be mediated by binding of the probes to the biofilm constituents through physicochemical interactions, essentially electrostatic and Lewis acid–base interactions, as already observed in different eukaryotic living cells [9,15,18]. Micro-electrophoresis measurements of the latex beads revealed their anionic nature with a zeta potential of -51 ± 5 mV at the pH of the study (pH = 6.0). This anionic character was the consequence of the prevalence of the deprotonated form of the carboxylate groups on the beads surface ($\text{p}K_a < 4$), which also precludes hydrogen-bond formation at pH 6.0. Considering that *S. maltophilia* bacteria are also negatively charged (-7 ± 3 mV at pH 6.0) [8], the electrostatic immobilization of the fluorescent probes within biofilms was very constrained.

Given the higher density of EPS in the mushroom-like structure compared to the homogeneous zone 1, an increased viscosity might have been expected, resulting in a parallel shift of the fluorescence correlation curve toward longer times (Fig. 3). However, the curve measured in zone 2 could not be superposed upon those obtained for the anionic latex beads in media with controlled viscosity [8]. Thus, with regard to the behaviour of the latex beads inside the mushroom structure, its diffusion can be only described as anomalous. The ap-

Table 1

Translational diffusion time τ_D and d_w parameters obtained from the fitting with Eq. (4) of the correlation curves of the fluorescent probes in the two distinct structural zones of *Stenotrophonas maltophilia* biofilm

Fluorophore	Zone 1		Zone 2	
	τ_D (ms)	d_w	τ_D (ms)	d_w
Carboxylated modified latex beads	13 ± 1	2.0	23 ± 7	2.5–2.9
Fluorescent labelled bacteriophages	123 ± 15	2.5–2.9	130 ± 10	3.0–3.4

parent diffusion coefficient obtained in this case was $D = 1.5 \mu\text{m}^2 \text{s}^{-1}$ ($\tau_D = 23$ ms) with a mean d_w value of 2.7 (Table 1). A previous study revealed, by contrast, diffusion inhibition for such large anionic latex beads in the mushroom-like structure of *Stenotrophonas maltophilia* biofilm grown in static conditions [8]. This apparent contradiction stresses out the dramatic influence of the biofilm growth mode on the diffusion processes.

Reasons for a non-Brownian diffusion of particles inside a biofilm can be only speculated. However, it should not be surprising that environmental heterogeneities (c.a. rafts, EPS density, water channels...) or local confinement can occur in the mushroom-like biofilm structure.

3.2.2. Fluorescent labelled bacteriophages

Fluorescent correlation curve profiles obtained for the labelled bacteriophages were markedly dependent upon local biofilm structure. Within more homogeneous structure (zone 1), the fluorescence correlation curves were already distorted in comparison with that obtained for free bacteriophages. These distortions increased with the compactness of local biofilm structure. Fig. 4 provides a series of fluorescent correlation curves at different depths within a mushroom-like region (zone 2) of the biofilm, nonetheless revealing any significant difference in all the bulk of the mushroom structure.

No inhibition of the viral particle diffusion was observed, but it appears complex in each part of the biofilm and requires to be analysed considering its intrinsic properties. As mentioned previously, the *Stenotrophonas maltophilia* bacteria are not sensitive to the C2 phages, precluding specific interaction between the two particles. Moreover, a viral particle can be considered as a biocolloid able to exchange physicochemical interactions with the surrounding medium. However, the bacteriophage immobilization inside the biofilm matrix due

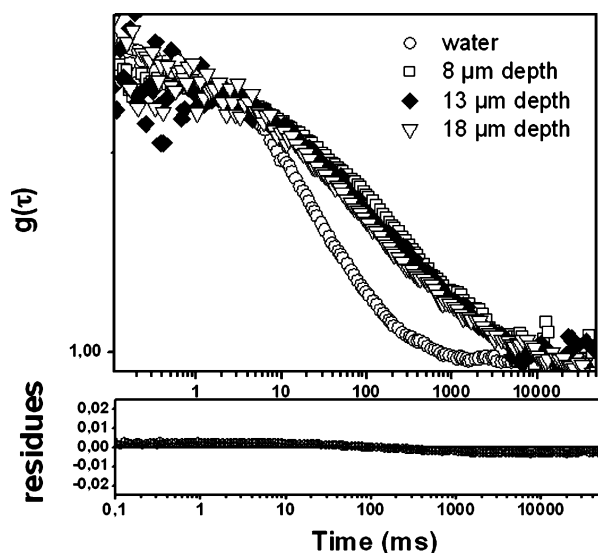


Fig. 4. Comparison of the fluorescence correlation curves for the labelled bacteriophages in water and at different depths of the mushroom-like structure of the biofilm (zone 2). The depth was expressed in μm from the glass cover slit surface. The fitting of the curves in zone 2 of the biofilm was obtained using Eq. (4).

to electrostatic interactions should be also reasonably excluded as for the reference latex bead. Indeed, the electrophoretic mobility measurement reveals a global negative charge of the phage surfaces with a zeta potential of -29 mV. Thus, the mobility of the C2 bacteriophages can be termed truly anomalous and the correlation curves satisfactorily fitted using Eq. (4). The experimental τ_D and d_w values are summarized in Table 1. We find for zones 1 and 2 comparable data for τ_D corresponding to a mean diffusion coefficient $D = 0.3 \mu\text{m}^2 \text{s}^{-1}$. The ratio of diffusion coefficients for the C2 bacteriophages and the reference latex beads was ~ 3 in water and reached ~ 10 in zone 1 of *Stenotrophonas maltophilia* biofilm. Owing to the absence of viscosity change in this part of the biofilm (see above), the slowing down of the diffusion could be related to the C2 phage morphology and specially its long tail. Furthermore, in both cases of latex beads and bacteriophages, the d_w values increase with the compactness of the medium (Table 1), emphasizing the role of EPS in diffusion.

4. Biological relevance

From a biological point of view, it has been previously hypothesized that the synergetic action of the bacteria in producing EPS may protect the majority of the biofilm occupant from infectious phage [19,20] or that bacteriophage migration through mucoid biofilms

was governed through a reduction in EPS viscosity by enzymatic degradation [6,21]. Our in situ experimental measurements suggest that, even in the absence of specific enzymatic reactions (no local viscosity change detected), viral particles can penetrate inside the EPS structure of mucoid biofilms. After penetration inside the polymeric matrix, the biological particle may then take advantage from the specific 'biofilm lifestyle', and in particular benefit from protection against 'outside' environmental stresses, such as desiccation or the action of antimicrobial agents. Bacterial cells present in a bacterial biofilm are typically 1000 times more resistant to antibiotics than they planktonic counterparts [2]. During biofilm erosion or sloughing, these protected immobilized viral particles may be released in the environmental fluid, and be in contact with their target hosts for a viral infectious cycle. Previous studies have demonstrated that immobilized viral particles on solid surface most often keep their infectious potential after desorption [22]. Interactions of pathogenic viruses with bacterial biofilm are also consistent with previous studies reporting the persistence of enteric virions or poliovirus-1 in microbial biofilm [23–25].

From a public health point of view, biofilms were already regarded as a common cause of bacterial infections. They should now also be considered as protective reservoirs of pathogenic viral particles, and are probably responsible for numerous persistent viral infections.

Acknowledgements

The authors would like to thank H. Bidnenko and S. Kulakauskas for their expertise in handling lactic acid bacteria bacteriophages and the French department of Essonne for its financial support for the purchase of a laser confocal microscope (ASTRE No. A02137).

References

- [1] J.W. Costerton, K.J. Cheng, G.G. Geesey, T.I. Ladd, N.C. Nickel, M. Dosgupton, I.J. Marine, Bacterial biofilms in nature and disease, *Annu. Rev. Microbiol.* 41 (1987) 4635–4641.
- [2] E. Licking, Getting a grip on bacterial slim, *Business Week* (13 September 1999) 98–100.
- [3] J.W. Costerton, P.S. Steward, E.P. Greenberg, Bacterial biofilms: a common cause of persistent infections, *Science* 284 (1999) 1318–1322.
- [4] B. Christensen, C. Sternberg, J.B. Andersen, L. Eberl, S. Moller, M. Givskov, S. Molin, Establishment of new genetic traits in a microbial biofilm community, *Appl. Environ. Microbiol.* 64 (1998) 2247–2255.
- [5] J.R. Lawrence, G.M. Wolfaardt, D.R. Korber, Determination of diffusion coefficients in biofilm by confocal laser microscopy, *Appl. Environ. Microbiol.* 60 (1994) 1166–1173.

- [6] G.W. Hanlon, S.P. Denyer, C.J. Olliff, L.J. Ibrahim, Reduction in exopolysaccharide viscosity as an aid to bacteriophage penetration through *Pseudomonas aeruginosa* biofilms, *Appl. Environ. Microbiol.* 67 (2001) 2746–2753.
- [7] P. Schwille, J. Korlach, W.W. Webb, Fluorescence correlation spectroscopy with single molecule sensitivity on cell and model membranes, *Cytometry* 36 (1999) 176–182.
- [8] E. Guiot, P. Georges, A. Brun, M.-P. Fontaine-Aupart, M.-N. Bellon-Fontaine, R. Briandet, Heterogeneity of diffusion inside microbial biofilms determined by fluorescence correlation spectroscopy under two-photon excitation, *Photochem. Photobiol.* 75 (2002) 570–578.
- [9] E. Hausteijn, P. Schwille, Ultrasensitive investigations of biological systems by fluorescence correlation spectroscopy, *Methods* 29 (2003) 153–166.
- [10] H.C. Chang, C.R. Chen, J.W. Lin, G.H. Shen, K.M. Chang, Y.H. Tseng, S.F. Weng, Isolation and characterization of novel giant *Stenotrophomonas maltophilia* phage phiSMA5, *Appl. Environ. Microbiol.* 71 (2005) 1387–1393.
- [11] D. Davies, M.R. Parsek, J.P. Pearson, B.H. Iglewski, J.W. Costerton, E.P. Greenberg, The involvement of cell-to-cell signals in the development of a bacterial biofilm, *Science* 280 (1998) 295–298.
- [12] M.W. Lubbers, N.R. Waterfield, T.P.J. Beresford, R.W.F. Le Page, A.W. Jarvis, Sequencing and analysis of the prolate-headed lactococcal bacteriophage C2 genome and identification of the structural genes, *Appl. Environ. Microbiol.* 61 (1995) 4348–4356.
- [13] B.E. Terzaghi, W.E. Sandine, Improved medium for lactic streptococci and their bacteriophages, *Appl. Environ. Microbiol.* 29 (1975) 807–813.
- [14] E. Guiot, M. Enescu, B. Arrio, G. Johannin, G. Roger, S. Tosti, F. Tifibel, F. Mérola, A. Brun, P. Georges, M.-P. Fontaine-Aupart, Molecular dynamics of biological probes by fluorescence correlation microscopy with two-photon excitation, *J. Fluorescence* 10 (2000) 413–419.
- [15] M. Wachsmuth, W. Waldeck, J. Langowski, Anomalous diffusion of fluorescent probes inside living cell nuclei investigated by spatially-resolved fluorescence correlation spectroscopy, *J. Mol. Biol.* 298 (2000) 677–689.
- [16] E.V. Craenenbroeck, Y. Engelborghs, Fluorescence correlation spectroscopy: molecular recognition at the single molecule level, *J. Mol. Recognit.* 13 (2000) 93–100.
- [17] J.R. Lawrence, D.R. Korber, B.D. Hoyle, J.W. Costerton, D.E. Caldwell, Optical sectioning of microbial biofilms, *J. Bacteriol.* 173 (1991) 6558–6567.
- [18] K.M. Berland, P.T.C. So, E. Gratton, Two-photon fluorescence correlation spectroscopy: method and application to the intracellular environment, *Biophys. J.* 68 (1995) 694–701.
- [19] K.A. Hugues, I.W. Sutherland, M.V. Jones, Biofilm susceptibility to bacteriophage attack: the role of phage-borne polysaccharide depolymerase, *Microbiology* 144 (1998) 3039–3047.
- [20] K.A. Hughes, I.W. Sutherland, J. Clarks, M.V. Jones, Bacteriophage and associated polysaccharide depolymerases – novel tools for study of bacterial biofilms, *J. Appl. Microbiol.* 85 (1998) 583–590.
- [21] I.W. Sutherland, K.A. Hugues, L.C. Skillman, K. Tait, The interaction of phage and biofilms, *FEMS Microbiol. Lett.* 232 (2004) 1–6.
- [22] S.S. Thompson, M. Flury, M.V. Yates, W.A. Jury, Role of air–water–solid interface in bacteriophage sorption experiments, *Appl. Environ. Microbiol.* 64 (1998) 304–309.
- [23] M.V. Storey, N.J. Ashbolt, Enteric virions and microbial biofilms – a second source of public health concern?, *Water Sci. Technol.* 48 (2003) 97–104.
- [24] J. Langmark, M.V. Storey, N.J. Ashbolt, T.A. Stenstrom, Accumulation and fated of microorganisms and microspheres in biofilms formed in a pilot-scale water distribution system, *Appl. Environ. Microbiol.* 71 (2005) 706–712.
- [25] F. Quignon, M. Sardin, L. Kiene, L. Schwartzbrod, Poliovirus-1 inactivation and interaction with biofilm: a pilot scale study, *Appl. Environ. Microbiol.* 63 (1999) 978–982.